Design of $\mathcal{L}1$ -Adaptive Controller for Single Axis Positioning Table

Amjad Jalil Humaidi
Assistant Professor. Dr.
Control and System Engineering Department-University of Technology
601116@uotechnology.edu.iq

Mohammed Ali Saffah Mohammed
Assist lecturer
Almansour College
mohammadalisffah@yahoo.com

Mohanad N. Mustafa
Assist lecturer
Control and System Eng. Dep. -University of Technology
Moohanadnm72@yahoo.com

ABSTRACT

L1 adaptive controller has proven to provide fast adaptation with guaranteed transients in a large variety of systems. It is commonly used for controlling systems with uncertain time-varying unknown parameters. The effectiveness of $\mathcal{L}1$ adaptive controller for position control of single axis has been examined and compared with Model Reference Adaptive Controller (MRAC). The Linear servo motor is one of the main constituting elements of the x-y table which is mostly used in automation application. It is characterized by time-varying friction and disturbance.

The tracking and steady state performances of both controllers have been assessed for two different types of input signals ramp and step inputs. The simulated results based on MATLAB (2012a) package showed that $\mathcal{L}1$ adaptive controller could outperform MRAC in terms of robustness and tracking.

Keywords: $\mathcal{L}1$ adaptive controller, position control, servo motor, x-y table

تصميم مسيطر متكيف نوع $\mathcal{L}1$ للسيطرة على الحركة الخطية لمحور لمنضدة ذات محور مفرد

امجد جليل حميدي
استاذ مساعد دكتور
قسم هندسة السيطرة والنظم ــ الجامعة التكنولوجية

مهند نوفل مصطفى
مدرس مساعد
قسم هندسة السيطرة والنظم ــ الجامعة التكنولوجية

محمد علي سفاح محمد
مدرس مساعد
كلية المنصور الجامعة

الخلاصة

في هذا العمل تم استخدام محرك مؤازر ذو تيار مستمر لتطبيق الحركة الخطية لمنضدة X-Y باتجاه محور واحد وقد تم استخدام مسيطر متكيف حديث (المسيطر المتكيف نوع $\mathcal{L}1$) المستخدم في السيطرة على المنظومات ذات المعلمات المتغيرة زمنيا والمجدولة القيمة. ولغرض المقارنة وتقييم الأداء تمـــــت مقارنة المسيطر المقترح (المسيطر المتكيف نوع $\mathcal{L}1$ مع المسيطر المتـــــكيف ذو المرجـــــــعية المـنمذجة (Model Reference Adaptive Control) وذلك للسيطرة على الموقع الخطي لمحورالمنضدة اليها. تم تقييم متانة المسيطرين اعلاه لمختلف انواع اشارات الادخال ومختلف التراكيب الغير مؤكدة (Uncertainties).

تم تنفيذ المحاكاة للمحركات الخطية المقترحة بوجود الاضطرابات وتراكيب الاحتكاك المتغيرة وتحت اشراف المسيطرين وذلك لاثبات الاساس النظري. اثبتت النتائج النظرية باستخدام برنامج (MATLAB 2012a) بأن المسيطر المتكيف نوع L_1 اعطى اداء متابعة واداء حركي داينميكي وخواص الحالة المستقرة افضل من تلك التي تم الحصول عليها من المسيطر المتكيف ذو المرجعية المنمذجة.

الكلمات الرئيسية: المسيطر المتكيف نوع $\mathcal{L}1$ ، السيطرة على الموقع ، محرك مؤازر ذو تيار مستمر ، منضدة X-Y.

1. INTRODUCTION

Over the last few years, $\mathcal{L}1$-adaptive control theory has attracted the attention of many control researchers. It permits transient characterization, cope with time varying uncertainties, and can create a compromise between tracking performance and robustness, **Hovakimyan, 2010**, and **Cao, 2009**.

$\mathcal{L}1$-adaptive control theory allows for decoupling of adaptation from robustness. The architecture also allows for transient characterization and robustness in the presence of fast adaptation without using persistent excitation, applying gain scheduling, or using high-gain feedback. Moreover, L_1-adaptive control can be used for nonlinear time-varying systems in the presence of state constraints, **Hovakimyan, 2010**, and **Hacker, 2011**.

To achieve its goals, L_1-adaptive control uses three distinct laws; state predictor law, adaptation law and control law. The state predictor law is responsible for modelling the system's desired performance, while the adaptation law ensures that the state estimates and plans are identical. Additionally, the control law tries to reduce the chattering in the control loop by including a low pass linear filter.

The $\mathcal{L}1$ controller has already been shown to be beneficial in many control applications such as drilling systems, wing rock, aerial vehicles, acrobats, the hysteresis in smart materials, and the regulation of arterial CO_2 tension in blood, **Techy, et al.**, **2007**, and **Pomprapa, et al**., **2013.**

In the present work, two controllers have been suggested, $\mathcal{L}1$ controller and Model Reference Adaptive Controller for positioning control of single axis positioning table. The performance comparisons of the presented controllers are assessed, via simulation, in terms of tracking and robustness.

2. ANALYSIS OF L_1-ADAPTIVE CONTROL

Two different architectures of adaptive control will be studied: Direct MRAC and Direct MRAC with state predictor which can be developed later to synthesize $\mathcal{L}_1$-adaptive control architecture. It is worthy to mention that L_1-adaptive control is a modified version of direct MRAC. Therefore, one can proceed to analyze the MRAC and then to state the main constructing elements of $\mathcal{L}1$ –adaptive control.

2.1 Direct Model Reference Adaptive Control (MRAC)

Let the system dynamics obey to the following structure of differential equation, **Hovakimyan, 2010**:

$$\dot{x}(t) = A_m x(t) + b\left(u(t) + k_x^{\mathrm{T}} x(t)\right), \quad x(0) = x_0 \tag{1}$$

$$y(t) = c^{\mathrm{T}} x(t)$$

where $x(t) \in \mathbb{R}^n$ is measured state of the system, $A_m \in \mathbb{R}^{n \times n}$, a known Hurwitz matrix, defines the desired dynamics for the closed-loop system and its eigenvalues should have negative real values, $b, c \in \mathbb{R}^n$ are known constant vectors, , $u(t) \in \mathbb{R}$ is the control input, $y(t) \in \mathbb{R}$ is the regulated output, and $K_x \in \mathbb{R}^n$ is a vector of unknown uncertainty constant parameters. The development of MRAC architecture is initiated by suggesting the nominal controller;

$$u_{nom} = -k_x^{\mathrm{T}} x(t) + k_g\, r(t) \tag{2}$$

where $r(t) \in \mathbb{R}$ is uniformly bounded piecewise-continuous reference input and k_g is given by

$$k_g \triangleq \frac{1}{c^T A_m^{-1} b} \tag{3}$$

The direct MRAC is given by

$$u(t) = -\hat{k}_x^T(t)x(t) + k_g\, r(t) \tag{4}$$

where $\hat{k}_x(t) \in \mathbb{R}^n$ is the estimate of k_x. Substituting Eq.(4) into Eq.(1) yields the closed – loop system dynamics, **Hovakimyan, 2010**:

$$\dot{x}(t) = \left(A_m - b\,\tilde{k}_x^T(t)\right)x(t) + b\,k_g r(t), \quad x(0) = x_0 \tag{5}$$

$$y(t) = c^T x(t)$$

where $\tilde{k}_x(t) \triangleq \hat{k}_x(t) - k_x$ denotes the parametric estimation error. The signal of tracking error will be:

$$e(t) \triangleq x_m(t) - x(t)$$

$$\dot{e}(t) = A_m\, e(t) + b\,\tilde{k}_x^T(t)x(t), \qquad e(0) = 0. \tag{6}$$

The updated law of the parametric estimate is given by **Cao, 2009**, and **Maalouf, 2013**:

$$\dot{\hat{k}}_x(t) = -\Gamma\, x(t)e^T(t)\, Pb, \qquad \hat{k}_x(0) = k_{x0} \tag{7}$$

where $\Gamma \in \mathbb{R}^+$ is the adaptation gain. The matrix $P = P^T > 0$ is found by solution of the algebraic Lyapunov equation, **Hacker, 2011**, and **Hovakimyan, 2007**:

$$A_m^T\, P + P\, A_m = -Q \tag{8}$$

For arbitrary $Q = Q^T > 0$. The block diagram of the closed–loop system is in **Fig.1**.

The following is the candidate of Lyapunov function:

$$V\left(e(t), \tilde{k}_x(t)\right) = e^T(t)\, P\, e(t) + \frac{1}{\Gamma}\, \tilde{k}_x^T(t)\, \tilde{k}_x(t) \tag{9}$$

Its time derivative along the system trajectories Eq.(6) – Eq.(7) is given by

$$\dot{V}(t) = -e^T(t)\, Q\, e(t) \leq 0. \tag{10}$$

Hence, the equilibrium of Eq.(6) and Eq.(7) is Lyapunov stable. The asymptotical convergence to zero of tracking error, the second derivative of Eq.(9) is used;

$$\ddot{V}(t) = -2e^T(t)Q\,\dot{e}(t). \tag{11}$$

It follows that $\dot{e}(t)$ is uniformly bounded, and hence $\ddot{V}(t)$ is bounded, implying that $\dot{V}(t)$ is uniformly continuous. Application of Barbalat's lemma yields, **Hovakimyan, 2010**:

$$\lim_{t \to \infty} \dot{V}(t) = 0 \tag{12}$$

which leads to the fact $e(t) \to 0$ as $t \to \infty$. Thus, $x(t)$ asymptotically converges   to $x_m(t)$.

2.2 Direct MRAC with State Predictor

One can re-parameterize the above-discussed structure utilizing a state predictor as follows, **Hacker, 2011,** and **Hovakimyan, 2007**

$$\dot{\hat{x}}(t) = A_m\hat{x}(t) + b\left(u(t) + \hat{k}_x^T(t)x(t)\right), \quad \hat{x}(0) = x_0 \tag{13}$$

$$\hat{y}(t) = c^T\hat{x}(t),$$

where $\hat{x}(t) \in \mathbb{R}^n$ is the state of the predictor. By subtracting Eq.(1) from Eq.(13), the prediction error dynamics can be obtained,

$$\dot{\tilde{x}}(t) = A_m\,\tilde{x}(t) + b\,\tilde{k}_x^T(t)\,x(t), \quad \tilde{x}(0) = 0 \tag{14}$$

where $\tilde{x}(t) \triangleq \hat{x}(t) - x(t)$ and $\tilde{k}_x(t) \triangleq \hat{k}_x(t) - k_x(t)$. One may note that these error dynamics are equivalent to the error dynamics indicated in Eq. (6). Next, let the adaptive law for $\hat{k}_x(t)$ be given as

$$\dot{\hat{k}}_x(t) = -\Gamma\, x(t)\, \tilde{x}^T(t)\, P\, b \qquad \hat{k}_x(0) = k_{x0}. \tag{15}$$

This adaptive law is identical to Eq.(7) in its structure with an exception of replacing the tracking error $e(t)$ is by the prediction error $\tilde{x}(t)$. The Lyapunov function candidate is chosen as **Hovakimyan, 2010**, and **Maalouf, 2013**:

$$V\left(\tilde{x}(t), \tilde{k}_x(t)\right) = \tilde{x}^{\mathrm{T}}(t)\, P\, \tilde{x}(t) + \frac{1}{\Gamma}\, \tilde{k}_x^{\mathrm{T}}(t)\, \tilde{k}_x(t) \tag{16}$$

which leads to

$$\dot{V}(t) = -\tilde{x}^{\mathrm{T}}(t)\, Q\, \tilde{x}(t) \leq 0. \tag{17}$$

This means that both errors $\tilde{x}(t)$ and $\tilde{k}_x(t)$ are uniformly bounded. However, Barbalat's lemma cannot be applied to prove asymptotic convergence of $\tilde{x}(t)$ to zero without introducing the feedback signal $u(t)$. Moreover, the estimation error $\tilde{x}(t)$ can be kept uniformly bounded if both $x(t)$ and $\hat{x}(t)$ diverge at the same rate.

The closed–loop of state predictor would mimic the reference system **Hovakimyan, 2010** :

$$\dot{\hat{x}}(t) = A_m\hat{x}(t) + b\, k_g\, r(t), \qquad \hat{x}(0) = x_0 \tag{18}$$

$$\hat{y}(t) = c^{\mathrm{T}}\,\hat{x}(t)$$

Thereby, Barbalat's lemma can be included to deduce that $\tilde{x}(t) \to 0$ as $t \to \infty$. **Fig. 2** shows the block diagram of the direct MRAC with state predictor.

3 PROBLEM FORMULATIONS:

The class of system indicated in Eq.(1) can be extended to the following more general class, **Hovakimyan, 2010, Cao,** and **Hovakimyan, 2007,** and **Cao,** and **Hovakimyan, 2008**;

$$\dot{x}(t) = A_m\, x(t) + b\left(\omega\, u(t) + \theta^{\mathrm{T}}(t)\, x(t) + \sigma(t)\right),\; x(0) = x_0 \tag{19}$$

$$y(t) = c^{\mathrm{T}}x(t) \tag{20}$$

where $\theta(t) \in \mathbb{R}^n$ is a vector of time-varying unknown parameters, $\omega \in \mathbb{R}$ is an unknown constant with known sign, and $\sigma(t) \in \mathbb{R}$ accounts for input disturbances.

The control objective is to ensure that $y(t)$ tracks a bounded piecewise-continuous reference signal $r(t)$ using full-state feedback adaptive controller, **Hovakimyan, 2010**, and **Cao,** and **Hovakimyan, 2007,** and **Hovakimyan, 2007**.

4. $\mathcal{L}_1$-ADAPTIVE CONTROL ARCHITECTURE

In what follows, the elements of $\mathcal{L}_1$--adaptive controller will be explained. The controller comprises three main parts; state predictor, adaptation law and control law, **Hovakimyan, 2010**, and **Cao,** and **Hovakimyan, 2007**, and **Hovakimyan, 2007**.

4.1 State Predictor

The following state predictor will be considered:

$$\dot{\hat{x}}(t) = A_m\hat{x}(t) + b\left(\hat{\omega}(t)u(t) + \hat{\theta}^{\mathrm{T}}(t)x(t) + \hat{\sigma}(t)\right),\; \hat{x}(0) = x_0$$

$$\hat{y}(t) = c^{\mathrm{T}}\hat{x}(t) \tag{21}$$

which is a similar structure indicated in Eq.(20) except that the unknown parameters ω, $\theta(t)$, and $\sigma(t)$ are exchanged by their adaptive estimates $\hat{\omega}(t)$, $\hat{\theta}(t)$, and $\hat{\sigma}(t)$, respectively.

4.2 Adaptation Laws

The adaptive process is conducted by the projection-based adaptation laws:

$$\dot{\hat{\theta}}(t) = \Gamma\, \mathrm{Proj}\left(\hat{\theta}(t), -\tilde{x}^{\mathrm{T}}(t)Pbx(t)\right) \qquad \hat{\theta}(0) = \hat{\theta}_0,$$

$$\dot{\hat{\sigma}}(t) = \Gamma\, \mathrm{Proj}(\hat{\sigma}(t), -\tilde{x}^{\mathrm{T}}(t)Pb) \qquad \hat{\sigma}(0) = \hat{\sigma}_0, \tag{22}$$

$$\dot{\hat{\omega}}(t) = \Gamma \, \text{Proj}\left(\hat{\omega}(t), -\tilde{x}^{\text{T}}(t) P b u(t)\right) \qquad \hat{\omega}(0) = \hat{\omega}_0$$

where $\tilde{x}(t) = \hat{x}(t) - x(t)$, $\Gamma \in \mathbb{R}^+$ is the adaptation rate and $P = P^{\text{T}} > 0$ is the solution of the algebraic Lyapunov equation $A_m^{\text{T}} P + P A_m = -Q$ for arbitrary $Q = Q^{\text{T}} > 0$.

4.3 Control Law

The control signal is produced as the output of the following (feedback) system **Cao, and Hovakimyan2007,** and **Hovakimyan2010**:

$$u(s) = -k \, D(s) \left(\hat{\eta}(s) - k_g \, r(s)\right), \tag{23}$$

where $r(s)$ and $\hat{\eta}(s)$ are the Laplace transforms of $r(t)$ and $\hat{\eta}(t)$, respectively, where $\hat{\eta}(t)$ and k_g are given by:

$$\hat{\eta}(t) \triangleq \hat{\omega}(t) u(t) + \hat{\theta}^{\text{T}}(t) \, x(t) + \hat{\sigma}(t), \tag{24}$$
$$k_g \triangleq -1/c^{\text{T}} A_m^{-1} b;$$

where $k > 0$ and $D(s)$ are a feedback gain and a strictly proper transfer function leading to a strictly proper stable

$$C(s) \triangleq \frac{\omega k D(s)}{1 + \omega k D(s)} \qquad \forall \omega \in \Omega_0 \tag{25}$$

The DC gain is set at $C(0) = 1$. Choosing $D(s) = 1/s$ results in a simple first-order strictly proper $C(s)$ of the form

$$C(s) = \frac{\omega k}{s + \omega k} \tag{26}$$

letting $\theta \in \Theta$ gives, **Hacker, 2011,** and **Hovakimyan, 2010**:

$$L \triangleq \max_{\theta \in \Theta} \|\theta\|_1$$
$$H(s) \triangleq (s\mathbb{I} - A_m)^{-1} b \tag{27}$$
$$G(s) \triangleq H(s)\left(1 - C(s)\right)$$

The $\mathcal{L}_1$-adaptive controller is subjected to the following $\mathcal{L}_1$-norm condition:

$$\|G(s)\|_{\mathcal{L}_1} L \leq 1 \tag{28}$$

The main elements $\mathcal{L}_1$-adaptive control structure is illustrated in **Fig. 3**.

If $\theta(t)$ is a stationary parameter of fixed value, then the $\mathcal{L}_1$-norm condition can be further simplified. For the special choice of $D(s) = 1/s$, the closed-loop system matrix A_g is given by;

$$A_g \triangleq \begin{bmatrix} A_m + b\theta^{\text{T}} & b\omega \\ -k\theta^{\text{T}} & -k\omega \end{bmatrix}, \tag{29}$$

where A_g has to be Hurwitz with all its eigenvalues have negative real values for all $\theta \in \Theta$ and $\omega \in \Omega_0$. **Figu.4** shows the difference between $\mathcal{L}_1$–adaptive controller and MRAC archetechture.

5. PROJECTION OPERATOR

Consider a convex, compact set with a smooth boundary given by **Hovakimyan, 2010**, and **Maalouf, 2013**.

$$\Omega_c \triangleq \{\theta \in \mathbb{R}^n | f(\theta) \leq c\} \qquad 0 \leq c \leq 1, \tag{30}$$

where $f: \mathbb{R}^n \to \mathbb{R}$ is described by the following convex function:

$$f(\theta) = \frac{\theta^T \theta - \theta_{max}^2}{\varepsilon_\theta \, \theta_{max}^2} \ , \qquad 0 < \varepsilon_\theta \leq 1 \tag{31}$$

where θ_{max} is the norm bound confining the parameter vector θ, and ε_θ represents the convergence tolerance that the adaptive parameter is allowed to exceed compared to its maximum conservative value. If a special structure of the function $f(\theta) \leq 1$, which defines the boundaries of the outer set, then one can get that $\theta^T \theta \leq (1 + \varepsilon_\theta) \theta_{max}^2$.

The projection operator can be defined as**, Cao,** and **Hovakimyan, 2007,** and **Hovakimyan, 2010**:

$$Proj(\theta, y) \triangleq \begin{cases} y & if\ f(\theta) < 0, \\ y & if\ f(\theta) \geq 0\ and\ \nabla f^T y \leq 0, \\ y - \frac{\nabla f}{\|\nabla f\|}\langle \frac{\nabla f^T}{\|\nabla f\|}, y \rangle & if\ f(\theta) \geq 0\ and\ \nabla f^T y > 0, \end{cases} \tag{32}$$

To geometrically interpret the above equation, let us define a convex set Ω_o as

$$\Omega_o \triangleq \{\theta \in \mathbb{R}^n | f(\theta) \leq 0\} \tag{33}$$

and let Ω_1 represent another convex set such that

$$\Omega_1 \triangleq \{\theta \in \mathbb{R}^n | f(\theta) \leq 1\} \tag{34}$$

Also, let $\Omega_{\mathcal{A}}$ represents an annulus region defined by

$$\Omega_{\mathcal{A}} \triangleq \Omega_1 \setminus \Omega_o = \{\theta | 0 < f(\theta) \leq 1\} \tag{35}$$

Inside $\Omega_{\mathcal{A}}$ the projection algorithm subtracts a scaled component of y that is normal to boundary $\{\theta | f(\theta) = \lambda\}$. If the value of λ is set to zero ($\lambda = 0$), then the scaled normal component is 0. Also, if the value of λ is set to unity ($\lambda = 1$), then the component of y that is normal to the boundary Ω_1 is entirely subtracted from y such that $Proj(\theta, y)$ is tangent to the boundary $\{\theta | f(\theta) = 1\}$. Further explanation can be seen in **Fig. 5**, where θ^* denotes the true value of the parameter θ and belong to Ω_o, i.e. $\theta^* \in \Omega_o$.

6. MODELING OF SINGLE AXIS POSITIONING TABLE

Fig. 6 shows the typical elements in one axis. An incremental optical encoder with a resolution of $\pm 1\mu m$ can measure the worktable position. A servomotor through a ball screw drives the worktable or slide. Rotary bearings support the screw at both ends. Linear bearings support the nut along the displacement axis. The nut is constrained to rotate axially and when the ball screw is turning, a linear motion is imparted to the nut. Linear guide-way precisely constrains the movement of the positioning table to a single translational axis. The elasticity of system is mainly caused due to the ball screw; bearing supports, and flux coupling, **Raafat, 2011**, and **ZAN, 2006**. The conceptual model of the mechanical system is illustrated in **Fig. 7** .

The following assumptions on the physical system are considered to develop a simplified model, **ZAN, 2006**:
1. Dynamic friction can be ignored.
2. The ball screw is rigidly coupled to the motor shaft.
3. The compliance between the slide table position and the ball nut is negligible.

The equation of motion can be derived from the simplified model according to the second law of Newton's as follows, **Raafat, 2011**:

$$J\ddot{\theta}(t) + B_1\dot{\theta}(t) = T_m(t) - T_l(t) - T_d(t) \tag{36}$$

$$M\ddot{x}(t) + B_2\dot{x}(t) = F_l(t) = T_l(t)/l_p \tag{37}$$

where J is the rotational inertia which includes motor shaft, $\theta(t)$ is the angular position, $x(t)$ is the measured table linear position, $T_m(t)$ is the motor torque, $T_l(t)$ is the load torque, $T_d(t)$ is the torque due to disturbances, M is the mass, $F_l(t)$ is the equivalent force acting on the positioning table, the coupling, and ball screw mass inertias, B_1 is the viscous damping arises from the rotational bearing and ball nut (lumped together), l_p is the screw pitch transformation

factor (from rotational to linear motion) and B_2 is the mechanical damping due to linear bearings.

It is well known that the torque $T_m(t)$ is related to the motor current I by a proportionality torque constant K_T given by motor the equation.

$$T_m(t) = K_T I \qquad (38)$$

The control voltage is the actual input of the system. The servo amplifier receives the applied voltage and supplies the current to the motor to develop the required electro-mechanical torque. It is assumed that amplifier has fast response such that its dynamic can be ignored and it is designated by constant gain K_a only for a certain range of operating point. Therefore, the motor torque can be written as, **Raafat, 2011**:

$$T_m(t) = K_a K_T u(t) \qquad (39)$$

where u is the input voltage signal. Consequently, the equation of motion (36) will be :

$$(J/l_p) \ddot{x} + (B_1/l_p) \dot{x} = K_a K_T u - l_p M \ddot{x} - l_p B_2 \dot{x} + f_{uc}(t) \qquad (40)$$

By regrouping the x terms in the left-half side, the equation can be expressed as follows:

$$\left(\frac{J + M l_p^2}{K_a K_T l_p}\right) \ddot{x} + \left(\frac{B_1 + B_2 l_p^2}{K_a K_T l_p}\right) \dot{x} = u + (1/K_a K_T) f_{uc}(t) \qquad (41)$$

where the uncertainty function $f_{uc}(t)$ accounts for nonlinear disturbances which includes the nonlinear friction, torque disturbances and other nonlinearities of the system,

$$f_{uc}(t) = f(v) + F_L \qquad (42)$$

$$f(v) = (F_s - F_c)sgn(v(t))e^{-(v(t)/v_s)^2} + F_c sgn(v(t)) \qquad (43)$$

where F_L is the load force and k_v is the coefficient of viscous friction. Equation (41) can be written as

$$M_x \ddot{x} + B_x \dot{x} = u + (1/K_a K_T) f_{uc}(t) \qquad (44)$$

where M_x and B_x can be given by:

$$M_x = \left(\frac{J + M l_p^2}{K_a K_T l_p}\right), \quad B_x = \left(\frac{B_1 + B_2 l_p^2}{K_a K_T l_p}\right)$$

Letting $x_1 = x$ and $x_2 = \dot{x}$ and Eq.(44) can be re-arranged to yield;

$$\dot{x}_2 = -(B_x/M_x) x_2 - (1/M_x) u - (1/M_x K_a K_T) f_{uc}(t) \qquad (45)$$

The state space form can be written in the following form;

$$\begin{bmatrix} \dot{x}_1 \\ \dot{x}_2 \end{bmatrix} = \begin{bmatrix} 0 & 1 \\ 0 & -\frac{B_x}{M_x} \end{bmatrix} \begin{bmatrix} x_1 \\ x_2 \end{bmatrix} + \begin{bmatrix} 0 \\ 1 \end{bmatrix} \left(\frac{1}{M_x} u - \frac{1}{M_x K_a K_T} f_{uc}(t)\right) \qquad (46)$$

$$y = [1 \quad 0] \begin{bmatrix} x_1 \\ x_2 \end{bmatrix},$$

If equation (46) had been compared with the following class of state equation,

$$\dot{x}(t) = A_m x(t) + b\left(\omega u(t) + \theta^T(t) x(t) + \sigma(t)\right)$$

By induction, one may easily find that

$$\omega = 1/M_x, \ \sigma(t) = -\frac{1}{M_x K_a K_T}(f(v) + F_L), \theta^T = [0 \quad -k_v/M_x],$$

$$b = [0 \quad 1]^T \text{ and } c = [1 \quad 0]$$

where $A_m = A - bK_m$ and $K_m = [k_1 \quad k_2]$ is the state feedback gain necessary for making the state matrix A being Hurwitz which all its eigenvalues have negative real values.

7. CONTROLLABILITY CONDITION FOR POLE-PLACEMENT

The requirement for applying pole placement is that the system must be completely stated controllable. The state space matrices for DC motor are given by:

$$A = \begin{bmatrix} 0 & 1 \\ 0 & -\frac{B_x}{M_x} \end{bmatrix} \text{ and } b = \begin{bmatrix} 0 & 1 \end{bmatrix}^T \tag{47}$$

which has the following parameters, **Raafat, 2011**:

$M_x = 0.0064$ and $B_x = 0.1966$

The controllability matrix is given by

$$\bar{M} = \begin{bmatrix} b & A\,b \end{bmatrix} = \begin{bmatrix} 0 & 1 \\ 1 & -\frac{B_x}{M_x} \end{bmatrix} \tag{48}$$

Also, it is clear that the controllability matrix has a rank equal to 2; i.e., the rank value is equal to system order and the DC-motor based system is said to be completely controllable. Substituting the numerical values of model parameters into state and input matrices, one can obtain,

$$A = \begin{bmatrix} 0 & 1 \\ 0 & -30.7692 \end{bmatrix} \quad , \quad b = \begin{bmatrix} 0 \\ 1 \end{bmatrix}$$

The eigenvalues for this system is $s_1 = 0$ and $s_2 = -30.7692$. Since the system has been shown to be completely state controllable, then the pole placement can be applied. If the desired eigenvalues are set as follows;

$\lambda_1 = -12.02$ and $\lambda_2 = -20.2$

The state feedback gain K_m which transfer the eigenvalues to desired location is given by

$K_m = \begin{bmatrix} k_1 & k_2 \end{bmatrix} = \begin{bmatrix} 242.804 & 1.4508 \end{bmatrix}$

This model matrix can be easily calculated as follows

$$A_m = A - b\,K_m = \begin{bmatrix} 0 & 1 \\ -242.804 & -32.22 \end{bmatrix}$$

8. STABILITY ANALYSIS OF $\mathcal{L}_1$-ADAPTIVE CONTROL FOR THE SINGLE-AXIS POSITIONING TABLE

In order to prove the system stability, the A_g matrix must be Hurwitz. Considering the values of the uncertainties in Tables1 and 3, the following matrices can be found:

$$A_m = \begin{bmatrix} 0 & 1 \\ -242.804 & -32.22 \end{bmatrix}, \; b = \begin{bmatrix} 0 \\ 1 \end{bmatrix}, \; \theta^T = \begin{bmatrix} 0 & -1.2521 \end{bmatrix}, \; \omega = 156.51077$$

Again, based on the simulation, $k = 100$. Substituting these parameters into the matrix A_g will produce the following matrix:

$$A_g = \begin{bmatrix} 0 & 1 & 0 \\ -242.804 & -33.4721 & 156.51077 \\ 0 & -125.21 & -15651.077 \end{bmatrix}$$

Using MATLAB package, the eigenvalues of matrix A_g is given by;

$\lambda_1 = -12, \; \lambda_2 = -20 \; , \; \lambda_3 = -15652$

Since all of these eigenvalues have negative real parts, this made A_g being Hurwitz and this will lead to the stability of overall system.

9. SIMULATED RESULTS OF SINGLE-AXIS POSITIONING TABLE

In what follows, the effectiveness of the two suggested controllers will be examined for different uncertainty structures and for different types of inputs. Table1 gives different uncertainty structure used in simulated results for various input types. If $f(v)$ is the friction force given by the following equation;

$$f(v) = (F_s - F_c)sgn(v(t)) \, e^{-(v(t)/v_s)^2} + F_c sgn(v(t)) \tag{49}$$

The values of friction parameters used in the simulation are given below, **ZAN, 2006.**

$k_v = 0.008 \; N.\,s/mm, \; F_c = \; 0.0008 \; N, \; F_s = 0.012 \; N, \; v_s = 0.0008 \; mm/s$

Other system parameters can are listed below, **Raafat, 2011**.

$M_x = 0.0064 \; kg, \; B_x = 0.1966 \; \text{kg/s}$

The form of the uncertainty $\sigma(t)$ becomes

$\sigma(t) = -(1/M_x K_a K_T)(f(v) + F_L)$

The other standard parameters are

$\theta^{\mathrm{T}} = [0 \quad -k_v/M_x], \; \omega = 1/M_x$

Using the numeric values, the range of compact set of $\sigma(t)$ for this application is given

$\sigma(t) \in \Delta = [-81.4939, 79.6953] \; N$

and the values of θ^{T} and ω are given, respectively, as

$\theta^{\mathrm{T}} = [0 \quad -1.2521], \; \omega = 156.25 \; (N/Amp.Kg)$

9. 1 Results based on ramp input

The behaviours of position and control signals for the single-axis system are reported based on different structures of uncertainties and under the supervision of two suggested controllers. The first structure of uncertainty is indicated as case (1) in Table 1. **Fig. 8** shows that $\mathcal{L}_1$-adaptive controller could keep good tracking performance giving a small value of steady state error (0.03) mm. On the other hand, MRAC could keep the tracking only for a period of time (2.4 sec), beyond which the system shows instability characteristics and the response would grow without limit. This is shown in **Fig. 9**.

For the uncertainty structure described in case (2) of Table 1, the system responses and control signals are shown in **Fig. 10** and **Fig. 11**. In case of **Fig. 10**, $\mathcal{L}_1$-adaptive controller still gives good tracking characteristics. However, the steady state error based on this controller is equal to $0.001mm$. Again, MRAC could only keep a tracking for a while as shown in **Fig. 11**. Beyond 2.4 sec., the response due to MRAC becomes unstable and the response would grow without bound.

The uncertainty structure of Case (3) will be considered. **Fig. 12**and **Fig. 13** show the position and control signal responses for both suggested controllers. The same discussion as the above can be argued with the exception that the steady state error resulting from $\mathcal{L}_1$-adaptive controller is equal to $0.03mm$. Also, the responses based on MRAC shows instability behavior after a period of time (2.4 sec.).

For the fourth case of Table 1**,** the responses and the control signals are shown in **Fig. 14**. Unfortunately, large steady state error are recorded for both controllers; as the value 0.25 mm is measured for the response based on $\mathcal{L}_1$-adaptive controller and the value 0.33 mm is measured for MRAC.

Table 2 lists the summary of steady state errors for all considered cases and for prescribed input. It is clear from the above scenarios that the steady state errors resulting $\mathcal{L}_1$-adaptive controller is much less than those resulting from MRAC.

9. 2 Results based on step input

In the next scenario, the uncertainty structures listed in Table 1 are reformulated and presented in Table 3. For the first case of Table 3, the responses and the control signals for bot controller are shown in **Fig. 15**. It is clear from the figure that $\mathcal{L}_1$-adaptive controller offers better tracking characteristics rather than MRAC. The steady-state error resulting from $\mathcal{L}_1$-adaptive controller is about $0.0076mm$, while that for the MRAC is $0.0329mm$.

For the uncertainty structure described in case (2) of Table 2, the responses and the control signals are shown in **Fig. 16**. Again $\mathcal{L}_1$-adaptive controller gives better tracking performance with smaller delay time than its counterpart. The steady-state error recorded for this scenario is 0.274 mm for $\mathcal{L}_1$-adaptive controller-based response and 0.4 mm for the MRAC-based response.

For the uncertainty structure depicted in case (3), the responses and the control signals for the suggested controllers are illustrated in **Fig. 17**. In case3, the disturbance amplitude was fixed, but the frequency was changed to 100 times of the first case. It is clear from the relative figure that the tracking performance given by $\mathcal{L}_1$-adaptive controller is better than the other one. Also, the steady-state error for $\mathcal{L}_1$-adaptive control response has been measured to be 0.0083 mm while that for the MRAC has been measured to be 0.025mm.

For the last case of Table 3, the responses and the control signals based on suggested controllers are shown in **Fig. 18**. In the present simulation, one can easily see that an oscillation would appear at the responses resulting from both controllers. However, at the steady state, low variance oscillation has been observed at the response resulting from $\mathcal{L}_1$-adaptive controller, while a considerable oscillation with large variance has appeared at the output resulting from MRAC. The steady state values given by $\mathcal{L}_1$-adaptive controller and MRAC are 0.0265 mm and 0.2774mm, respectively.

Table 4 gives the summary of different steady state errors for different cases. Again, the errors based on $\mathcal{L}_1$-adaptive controller are much less than those obtained from MRAC.
Table 5 shows the settling time for step input response of 5 mm. It can be noticed that the settling time of $\mathcal{L}_1$-adaptive controller for all considered cases are less than MRAC. This means that $\mathcal{L}_1$-adaptive controller has a faster adaptation rate than MRAC.

CONCLUSIONS

Based on observations of the simulated result, the following conclusions can be drawn:

1. For ramp exciting input, the results showed that $\mathcal{L}_1$-adaptive controller has better tracking performance than MRAC. However, for specified uncertainty structures, MRAC fails to follow ramp input after a short time. This leads to instability problems in MRAC and its corresponding response grows without bound.

2. For step exciting input, $\mathcal{L}_1$-adaptive controller could track and gives better transient characteristics than MRAC. However, for specified uncertainty structures, the response based on MRAC shows severe oscillatory characteristics.

3. In case of step input, it can be concluded that the settling time of the $\mathcal{L}_1$-adaptive controller for all cases of uncertainties is less than that of MRAC. This means that the adaptation rate of $\mathcal{L}_1$-adaptive controller is faster than that of MRAC.

4. Chattering shown in responses of positions occurred because of the presence of Signum function in the friction model.

REFERENCES

- Hovakimyan, N., 2010, *$\mathcal{L}_1$-Adaptive Control Theory Guaranteed Robustness with Fast Adaptation*, Society for Industrial and Applied Mathematics (SIAM) Philadelphia.

- Cao, C., 2009, *L1*-Adaptive Output Feedback Controller for Non Strictly Positive Real Reference Systems with Applications to Aerospace Examples, AIAA Guidance.

- Hacker, J. E., 2011**,** *L1*-Adaptive Control of Uncertain Nonlinear Systems with Dynamic Constraints" As Applied to Commercial Aircraft Engines, Master Thesis, University of Connecticut, Mechanical Engineering.

- Techy, L., Reddy, C. K., and frere, **C. A., C., N.,** 2007, Nonlinear Control of a Novel Two-Link Pendulum, American Control Conference, New York City, USA, pp. 19–24, July.

- Pomprapa, A., Walter M., and frere, C., B., S**.,** 2013, $\mathcal{L}1$ -Adaptive Control of end-tidal CO_2 by optimizing the muscular power for mechanically ventilated patients, 9th IFAC Symposiumon Nonlinear Control Systems, Toulouse, France, pp. 259–264.

- Maalouf D., 2013, Contributions to Nonlinear Adaptive Control of Low Inertia Underwater Robots, PhD Thesis, Universite Montpellier II, Sciences et Techniques du Languedoc.

- Cao C., and Hovakimyan N., 2007, Guaranteed Transient Performance with *L1* Adaptive Controller for Systems with Unknown Time varying Parameters and Bounded Disturbances, American Control Conference, New York City, USA, pp. 3925–3930.

- Cao C., and Hovakimyan N., 2008, $\mathcal{L}1$- Adaptive Controller for Systems with Unknown Time-Varying Parameters and Disturbances in the Presence of Non-zero Trajectory Initialization Error, International Journal of Control, Vol. 81, No. 7, pp. 1147-1161.

- Cao C., and Hovakimyan N., 2007, $\mathcal{L}1$- Adaptive Output Feedback Controller for Systems with Time-varying Unknown Parameters and Bounded Disturbances", American Control Conference, New York City, USA, pp. 486–491.

- Hovakimyan N., 2007, Stability Margins of *L1* Adaptive Controller: Part II", American Control Conference, New York City, USA, pp. 3931–3936.

- Raafat M. 2011, Intelligent Robust Control of Precision Positioning Systems Using Adaptive Neuro Fuzzy Inference System", PhD thesis, International Islamic University, Malaysia.

- BIN M. Z., ZAN M., 2006, Control Strategy Of A Ballscrew Driven Positioning Table In The Presence Of Friction, Master thesis, International Islamic University, Mechatronics Engineering, Malaysia.
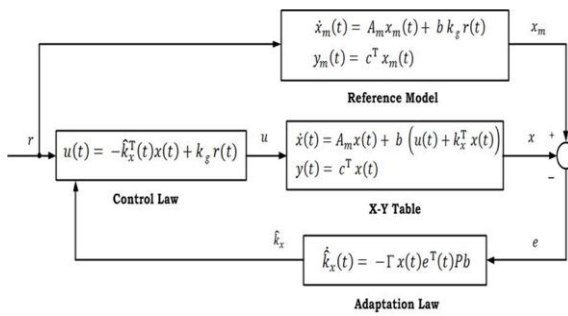
Figure 1. Closed-loop direct MRAC architecture
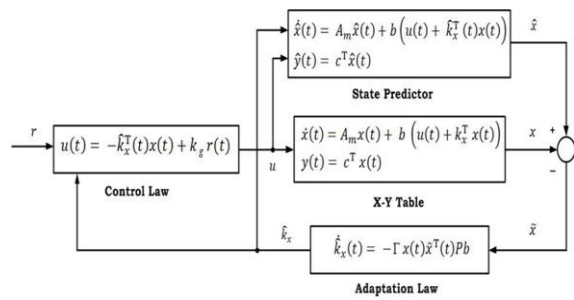
Figure 2. Closed-loop MRAC architecture with state Predictor
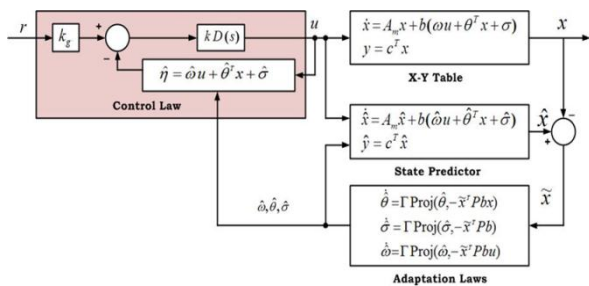
Figure 3. Closed-loop L_1-adaptive system
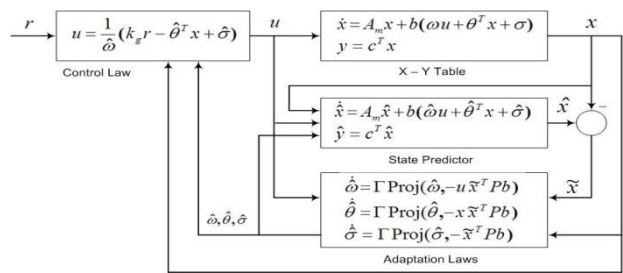
Figure 4. Closed-loop MRAC system
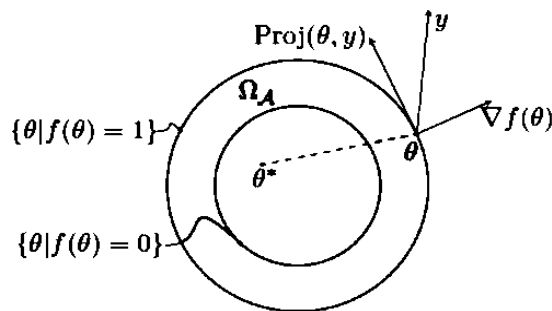
Figure 5. Visualization of Projection Operator in $\mathbb{R}^2$
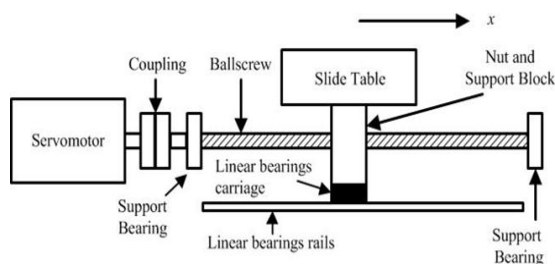
Figure 6. Elements of single axis positioning table.
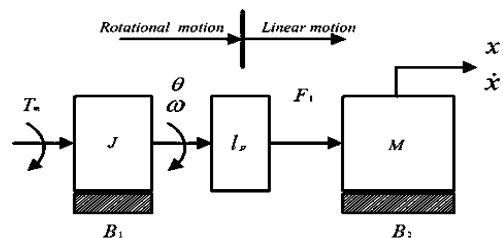
Figure 7. Simplified model of positioning table.
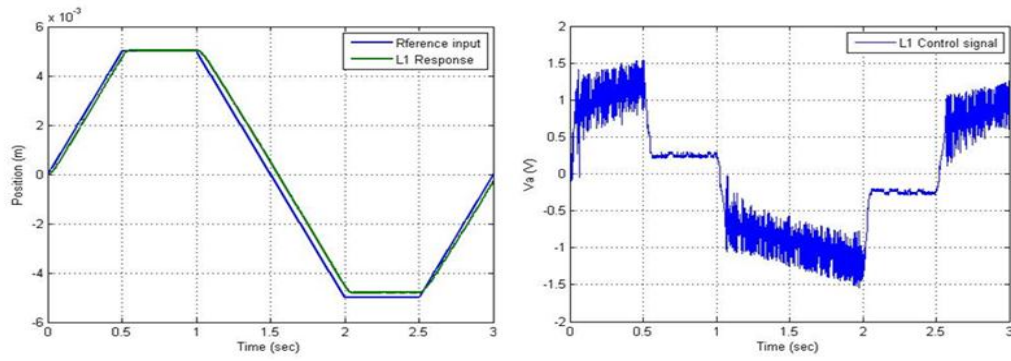
Figure 8. Transient responses based on L_1- adaptive controller for ramp input (case 1).
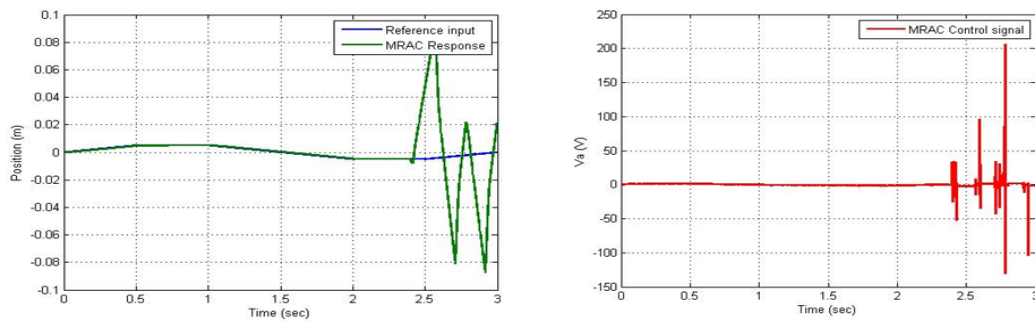
Figure 9. Transient responses based on MRAC for ramp input (case 1)
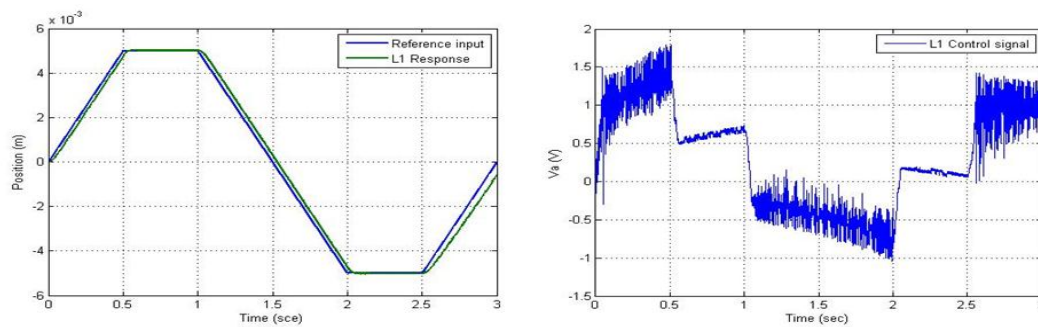
Figure 10. Transient response based on L_1- adaptive controller for ramp input (case 2).
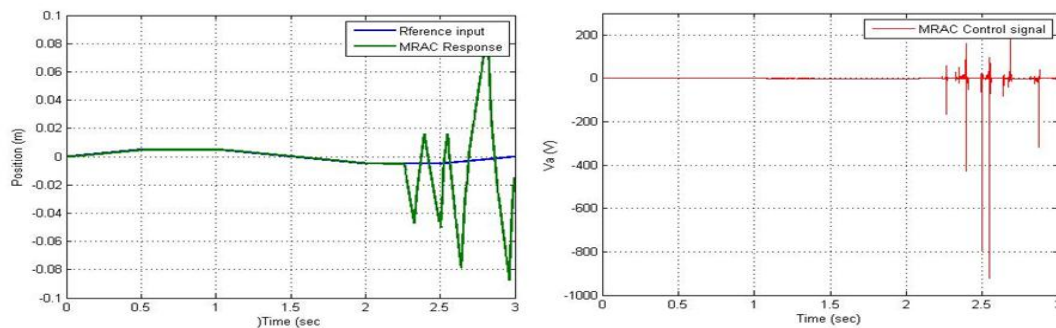
Figure 11. Transient response based on MRAC for ramp input (case 2).
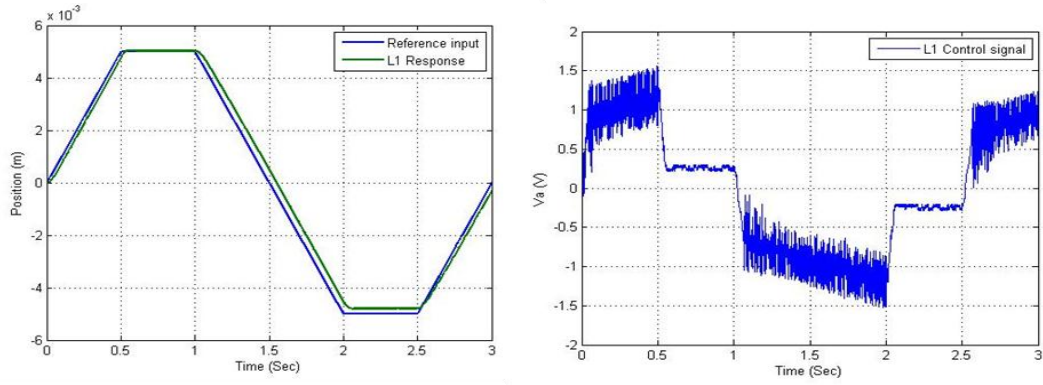
Figure 12. Transient response based on L_1 adaptive controller for ramp input (case 3).
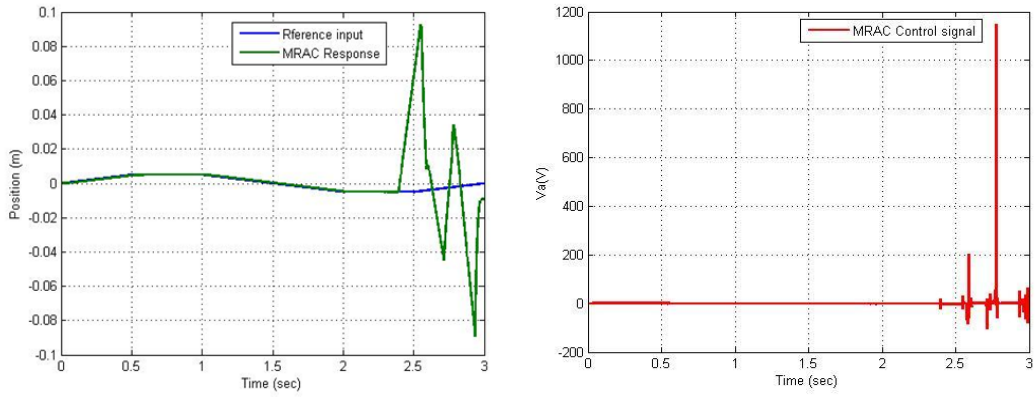
Figure 13. Transient response based on MRAC for ramp input (case 3).
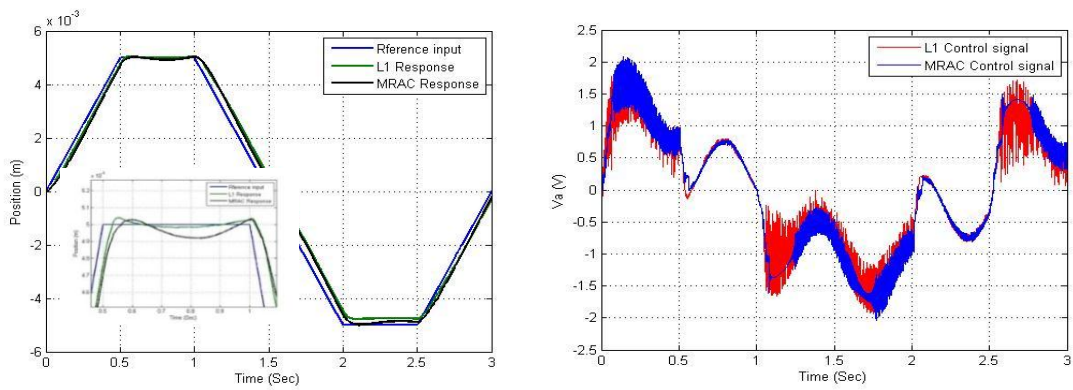
Figure 14. Transient response based on MRAC for ramp input (case 4).
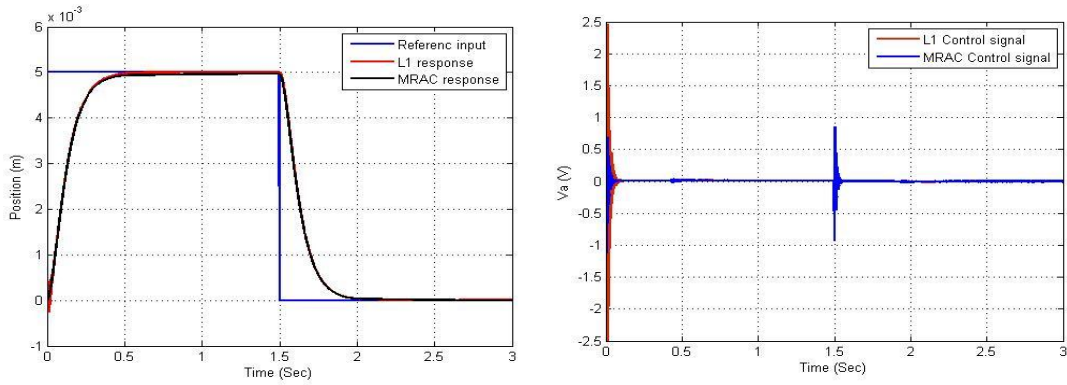
Figure 15. Transient responses based on L_1 adaptive controller and MRAC for step input (case 1).
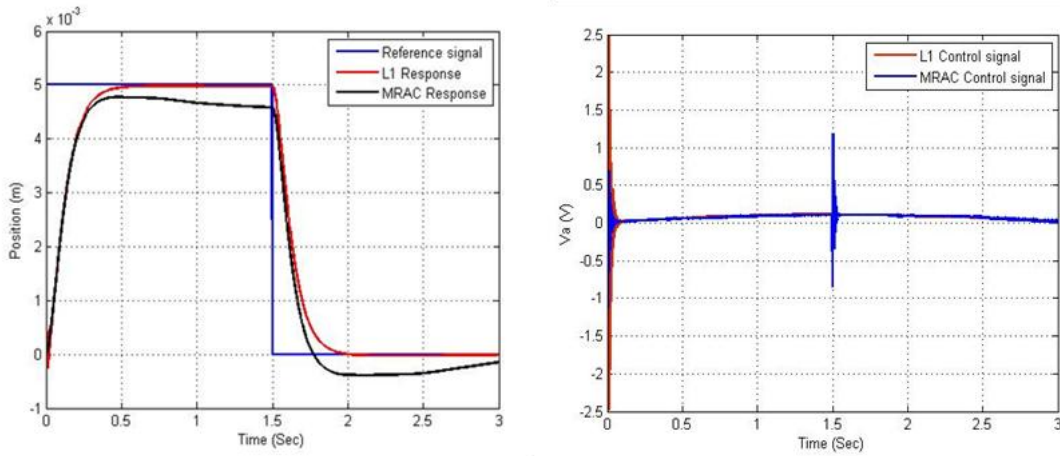
Figure 16. Transient responses based on L_1 adaptive controller and MRAC step input (case 2).
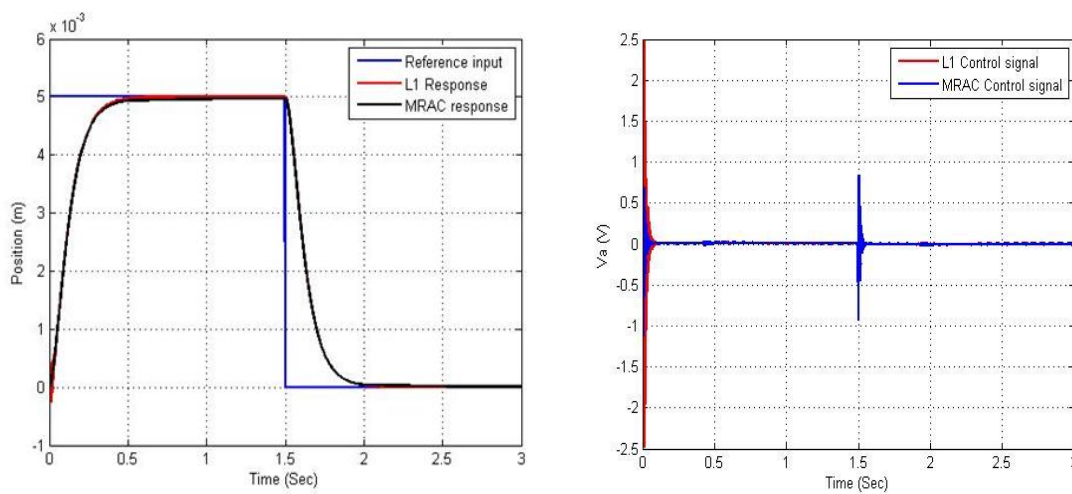
Figure 17. Transient responses based onL_1- adaptive controller and MRAC step input (case 3).
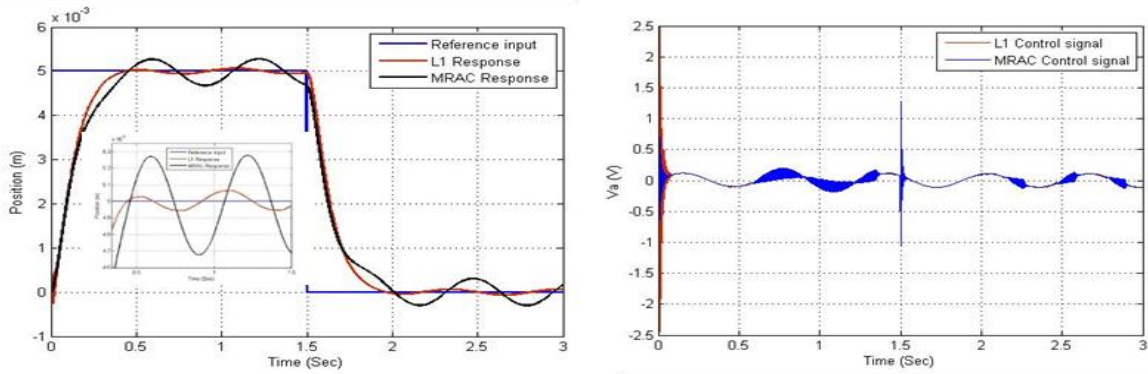
Figure 18. Transient based on L$_1$- adaptive controller and MRAC for step input (case 4).

Table 1. Structure of uncertainty.

Parameter	Case 1	Case 2	Case 3	Case 4
$\sigma(t)$	$0.002\sin(t)$ $+ f(v)$	$0.51\sin(t)$ $+ f(v)$	$0.002\sin(10t)$ $+ f(v)$	$0.51\sin(10t)$ $+ f(v)$

Table 2. Steady-state errors for different cases.

	Steady state error (mm)			
	Case 1	Case 2	Case 3	Case 4
$\mathcal{L}_1$-controller	0.03	0.001	0.03	0.25
MRAC	Undefined	Undefined	Undefined	0.33

Table 3. Structure of uncertainty for step input.

Parameter	Case 1	Case 2	Case 3	Case 4
$\sigma(t)$	$0.002\sin(t)$ $+ f(\theta)$	$0.11\sin(t)$ $+ f(\theta)$	$0.002\sin(100t)$ $+ f(\theta)$	$0.11\sin(10t)$ $+ f(\theta)$

Table 4. Steady-state errors for different cases of ramp input.

	Steady state error (mm)			
	Case 1	Case 2	Case 3	Case 4
L$_1$-controller	0.0076	0.274	0.0083	Un defined
MRAC	0.0329	0.4	0.025	Un defined

Table 5. Settling time for different cases of step input signal.

	Settling time (sec)			
	Case 1	*Case 2*	*Case 3*	*Case 4*
L$_1$-controller	0.76	0.7	0.75	0.6
MRAC	1	1.4	1.2	0.73